Polymer 51 (2010) 1395–1403

Contents lists available at ScienceDirect

Polymer

journal homepage: www.elsevier.com/locate/polymer

Ag nanoparticle/azopolymer nanocomposites: In situ synthesis, microstructure, rewritable optically induced birefringence and optical recording

Si Wu [a], Jing Shen [a,1], Jintang Huang [b,2], Yeping Wu [a], Zhoushun Zhang [a], Yanlei Hu [b], Wenxuan Wu [a], Wenhao Huang [b], Keyi Wang [b], Qijin Zhang [a,*]

[a] CAS Key Laboratory of Soft Matter Chemistry, Department of Polymer Science and Engineering, University of Science and Technology of China, Key Laboratory of Optoelectronic Science and Technology in Anhui Province, Hefei, Anhui 230026, PR China
[b] Department of Precision Machinery and Precision Instrumentation, University of Science and Technology of China, Hefei, Anhui 230026, PR China

ARTICLE INFO

Article history:
Received 28 September 2009
Received in revised form
22 January 2010
Accepted 29 January 2010
Available online 4 February 2010

Keywords:
Polymer nanocomposites
Azobenzene
Silver nanoparticle

ABSTRACT

Ag nanoparticle/azopolymer nanocomposites are prepared with controlled concentration of Ag nanoparticles by in situ reduction of Ag(I) β-diketone complexes in an azopolymer matrix. The nanocomposites form an organic–inorganic network-like structure by interactions between the azopolymer matrix and the Ag nanoparticles. The Ag/azopolymer nanocomposites are homogeneous and highly transparent even when the content of Ag is as high as 5.6 wt%. Birefringence of the azopolymer without Ag and the nanocomposites can be optically induced and erased. However, after 5 cycles of optically writing–erasing processes, 9.7% decrease of the birefringence is observed for the azopolymer film without Ag and only 2.9% decrease of the birefringence is observed for the nanocomposite film with 5.6 wt% Ag, showing the stability of photo-induced birefringence of the nanocomposite is improved by introducing Ag nanoparticles into the azopolymer matrix. Relatively high concentration of Ag nanoparticles does not strongly hinder the mobility of azobenzene groups during photoisomerization and one-photon recording. In two-photon optical recording experiments, an image on the nanocomposite with 5.6 wt% Ag can be observed with writing power as low as 6 mW and no such an image can be observed in the azopolymer without Ag under the same two-photon recording condition.

1. Introduction

Recent scientific researches have demonstrated that combining hard and soft materials can result in composites with improved stability and new functionalities [1–5]. Incorporating photochromic molecules into hybrid organic–inorganic materials leads to photoresponsive systems, the properties of which can be manipulated by light [6]. Azobenzene derivatives are photochromic molecules, which show reversible trans–cis isomerization under light irradiation [7–9]. Functional composite materials can be fabricated by combining azobenzene derivatives with inorganics [10–27]. In the past few years, many azobenzene/noble metal (Ag or Au) composites were fabricated and these composites showed novel properties [17–27]. On the one hand, the surface plasmon resonance (SPR) of noble metal nanoparticles have shown effects on the photochemical properties of azobenzene derivatives in the composites [17–22]; on the other hand, the reversible isomerization of azobenzene can be used to control the properties of noble metal nanoparticles by light, resulting in switchable nanocomposite systems [19,23–25]. For example, sub-diffraction imaging of the optical near-field in nanostructures is achieved based on the effect of SPR of noble metal nanostructures on the photosensitive azobenzene derivatives [17,28]; noble metal nanoparticles cause surface-enhanced Raman scattering (SER) of azobenzene derivatives [20–22]; photoisomerization of azobenzene derivatives can be used to control aggregated states, colors and SPR signals of noble metal nanoprticles [23,24]. These properties make azobenzene/noble metal composites promising materials as photoswitches, rewritable information storages, self-erasing materials, etc. [17–27].

The biggest problem that prevents the azobenzene/noble metal composites from real applications is how to fabricate homogenous azobenzene/noble metal composites with good processability and controllable concentration of noble metal nanoparticles. It is well known that polymers have good processability. If azobenzene-containing composites are embedded into a polymer matrix or

* Corresponding author. Tel./fax: +86 551 3601704.
E-mail address: zqjm@ustc.edu.cn (Q. Zhang).
[1] Current address: Institute of Textiles and Clothing, The Hong Kong Polytechnic University, Hong Kong
[2] Current address: Fraunhofer Institute for Laser Technology, Steinbachstraβe 15, 52074 Aachen, Germany

0032-3861/$ – see front matter © 2010 Elsevier Ltd. All rights reserved.
doi:10.1016/j.polymer.2010.01.062

nanoparticles are embedded into an azopolymer (a kind of polymer with azobenzene groups covalently linked to the polymer chain) matrix, composite materials with good processability can be obtained. Actually, several attempts were made to fabricate azobenzene/noble metal composites with good processability in this way [18,22,23]. Klajn et al. reported that they doped azobenzene/noble metal nanocomposites into a poly(methyl methacrylate) (PMMA) matrix [23]. Although the film-forming property of these composites is good, the concentration of noble metal nanoparticles in the composite films is very low [23]. Zhou et al. reported that they doped Ag nanoparticles with an average diameter of 10 nm into an azopolymer [18]. The Ag nanoparticles form aggregates of several hundred nanometers to several micrometers even when the concentration of Ag nanoparticles is lower than 0.1 wt% [18]. Gao et al. reported that they used an azopolymer with a terminal thiol group to graft the azopolymer onto Ag nanoparticles to form composites [22]. Although homogenous nanocomposites can be obtained in this way, this method needs a complex chemical synthesis; further more, each polymer chain has only one thiol group to protect the Ag nanoparticles so that nanocomposites with high concentration of Ag nanoparticles cannot be fabricated by this method [22]. Therefore, it is highly desirable to find an alternative method to fabricate homogenous azobenzene/noble metal composites with good processability and controllable concentration of noble metal nanoparticles.

The aim of this work is to demonstrate a new strategy to fabricate homogenous azopolymer/noble metal nanocomposites with good processability and controllable concentration of nanoparticles and study the optical properties of these polymer nanocomposites. Our strategy of fabrication such nanocomposites is based on in situ reduction of Ag(I) organic complex in an azopolymer matrix, which is shown in Scheme 1. Ag(I) organic complex has much better solubility in organic solvents and much better miscibility in the azopolymer matrix than inorganic Ag nanoparticles, so Ag(I) organic complex can be introduced into the azopolymer matrix homogenously and the content of Ag element in the precursor can be largely increased. Good films of the precursors can be fabricated by spin-coating or drop-casting and simply heating can lead to decomposition of the Ag(I) organic complex and formation of Ag nanoparticles. The interactions between the substituents of the azopolymer and Ag nanoparticles can prevent the Ag nanoparticles from aggregation. The Ag/azopolymer nanocomposites fabricated by in situ reduction are homogeneous and highly transparent even when the content of Ag is as high as 5.6 wt%. We also find Ag nanoparticles have effects on the optically induced birefringence and two-photon recording of azopolymer.

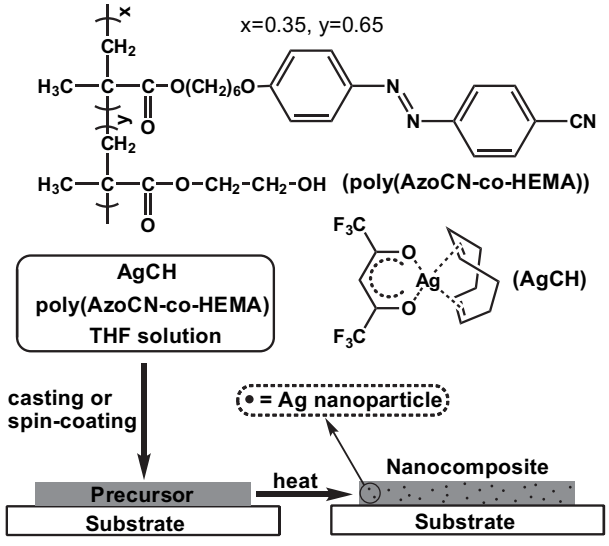

Scheme 1. Chemical structures of poly(AzoCN-co-HEMA) and AgCH; and the process of fabrication of Ag/azopolymer nanocomposites.

2. Experimental section

2.1. Materials

The chemical structures of the azopolymer and the Ag(I) complex are shown in Scheme 1. The Ag(I) complex (1,5-cyclooctadiene)-(hexafluoroacetylacetonato) Ag(I) (abbreviated as AgCH) was purchased from Aldrich. The azo monomer 6-(4-((4-cyanophenyl)diazenyl)phenoxy)hexyl methacrylate (abbreviated as AzoCN) was synthesized according to the previous work [29]. The azopolymer (abbreviated as poly(AzoCN-co-HEMA)) was synthesized by polymerization of AzoCN and 2-hydroxyethyl methacrylate (HEMA) and the detail of synthesis of poly(AzoCN-co-HEMA) is in the following way. 0.39 g (1 mmol) AzoCN, 0.195 g (1.5 mmol) HEMA and 20.5 mg 2, 2′-azobisisobutyronitrile (AIBN) were dissolved in 1.5 mL anhydrous tetrahydrofuran (THF). After 3 freeze–thaw cycles, the flask was sealed in a vacuum. Polymerization was conducted at 55 °C for 48 h. The obtained polymer was precipitated in methanol, and the purification was repeated three times in a THF/methanol system. The GPC measurement of average molecular weight and polydispersity are $M_n = 42{,}000$ and $M_w/M_n = 1.62$, respectively. The molar ratio of AzoCN and HEMA in the copolymer is 35% and 65%, respectively, which is calculated from the ^{1}H NMR spectrum.

2.2. Preparation of the nanocomposite films

The process of preparation of the nanocomposite films is shown in Scheme 1. We prepared the nanocomposites in the following way. 90 mg poly(AzoCN-co-HEMA) and calculated amount of AgCH were dissolved in 3 mL THF. The THF solutions were stirred for several hours before use. AgCH/azopolymer films (the precursors) were obtained by spin-coating or drop-casting from the THF solutions onto quartz, silicon wafer or glass substrates for different measurements. The films were dried in air over night. The nanocomposite films were obtained by heating the precursors at 95 °C under vacuum for 3 h. We prepared 4 samples with different AgCH concentrations. The composition of the precursors with different concentration of AgCH is shown in Table 1. The thickness of the films by spin-coating and drop-casting were estimated to be 1.4–1.5 μm and 3.2–3.5 μm, respectively, by the film thickness measurement software of our UV–vis absorption spectrophotometer.

2.3. Measurements

UV–vis absorption spectra were measured on an SHIMADZU UV-2550 PC spectrophotometer. X-ray photoelectron spectra (XPS) were measured on a VG ESCALAB MK-II photoelectron spectrometer using Mg $K_\alpha = 1253.6$ eV. FT-IR spectra were obtained using a Nicolet 8700 spectrometer. Microscopic images were obtained on

Table 1
The composition of the precursors.

Sample	AgCH (wt%)	Ag element (wt%)
Ag1	8.5	2.2
Ag2	12.8	3.3
Ag3	17.6	4.5
Ag4	21.9	5.6

an Olympus BX51 microscope. SEM images were obtained on a Sirion200 system. The morphology of the Ag nanoparticles was observed on a JEOL-2010 transmission electron microscope (TEM). The samples for the TEM measurements were prepared in the following way. The nanocomposite films were firstly stripped from the substrates and were dispersed in acetone by sonication, and then the samples for TEM measurements were obtained by applying a drop of the acetone dispersion onto a Cu grids and leaving it dry in air. Photoisomerization of azo chromophores were induced by a high-pressure mercury arc combined with a UV filter. The intensity of the UV light (~365 nm) was about 5.4 mW cm^{-2}. Optically induced and erased birefringence of the nanocomposite films were investigated on a setup reported in our previous work [30]. The birefringence of the films was induced by linearly polarized light (LPL) of a He–Cd laser at 442 nm with an intensity 309 mW cm^{-2}. The birefringence was optically erased by overwriting the samples with circularly polarized light (CPL) from the same He–Cd laser. The transmittance of the samples during the writing–erasing process was detected by a probe light at the same time. The probe light, polarized at 45° with respect to the polarization direction of the writing light and passed through a pair of crossed polarizers, was a low power diode laser at 650 nm. The transmittance change of the probe light was recorded and the signals were transmitted to a computer. One-photon recording was using a LABRAM-HR confocal microscope system. The system is equipped with a linearly polarized laser at 514.5 nm and a mobile sample stage. The diameter and intensity of the laser at the focal point were about 2 μm and 1 mW. Two-photon recording were using a linearly polarized Ti:Sapphire laser (wavelength: 800 nm, pulse duration: 80 fs, and repetition rate: 80 MHz). The detail of the experimental setup for two-photon recording was reported elsewhere [31].

3. Results and discussion

3.1. Characterization of Ag/azopolymer nanocomposites

It is known that Ag nanoparticles can be synthesized by decomposition of Ag(I) β-diketone complexes [32,33]. Preparation of the Ag/azopolymer composites is based on in situ reduction of the Ag (I) β-diketone complex AgCH. Four nanocomposites (Ag1, Ag2, Ag3 and Ag4, see Table 1) with different contents of Ag are obtained in this way. The formation of Ag nanoparticles in these composites is demonstrated by TEM analysis and UV–vis absorption spectroscopy.

Fig. 1 shows TEM images and the corresponding particle size distribution histograms of nanocomposites. Spherical Ag nanoparticles can be observed in all these samples. Particle size distribution histograms are obtained from statistic analysis on at least 250 particles. The average diameters of Ag nanoparticles calculated from the TEM images are 8.3 nm, 8.5 nm, 8.8 nm and 10.0 nm for Ag1, Ag2, Ag3 and Ag4, respectively. The average diameter of Ag nanoparticles increases as the concentration of AgCH in the precursor increases.

The photograph of the nanocomposite Ag4 is shown in Fig. 2(a). The film is homogeneous and highly transparent. It was reported that when Ag nanoparticles with an average diameter of 10 nm were doped into an azopolymer, Ag nanoparticles formed aggregates of several hundred nanometers to several micrometers [18]. To check if there are big aggregates of Ag nanoparticles in the in situ synthesized nanocomposite Ag4, the morphology of Ag4 is observed by optical microscopy and SEM. As shown in Fig. 2(b) and (c), Ag4 is homogeneous and without any big aggregates of Ag nanoparticles. The photograph of the azopolymer film without Ag is also shown in Fig. 2(a) for comparison. The color of the azopolymer film is yellow and the color of the nanocomposite Ag4 is brown. The different colors of the films with and without Ag nanoparticles are caused by the absorption of Ag nanoparticles in the visible range, which can be detected by UV–vis absorption spectroscopy.

UV–vis absorption spectra of the azopolymer and the nanocomposite films are shown in Fig. 3(a). There are two absorption bands in the absorption spectrum of the azopolymer. The band at about 358 nm is a strong one and the other band at about 455 nm is a weak one. They are ascribed to the π–π^* transition of trans azobenzene groups and n–π^* transition of cis azobenzene groups, respectively. It is well known that Ag nanoparticles have a characteristic surface plasmon resonance (SPR) band in the visible range [34–36]. For the nanocomposite films, the absorption band at about 455 nm increases as the content of Ag increases, indicating the SPR band of Ag nanoparticles is located at around 455 nm. The n–π^* transition of cis azobenzene group is also located at around 455 nm. So, the SPR band of Ag nanoparticles is overlapped with the n–π^* transition of cis azobenzene group in the visible range.

If the absorbance of the azopolymer is subtracted from the measured spectra, we obtain the SPR bands of Ag nanoparticles,

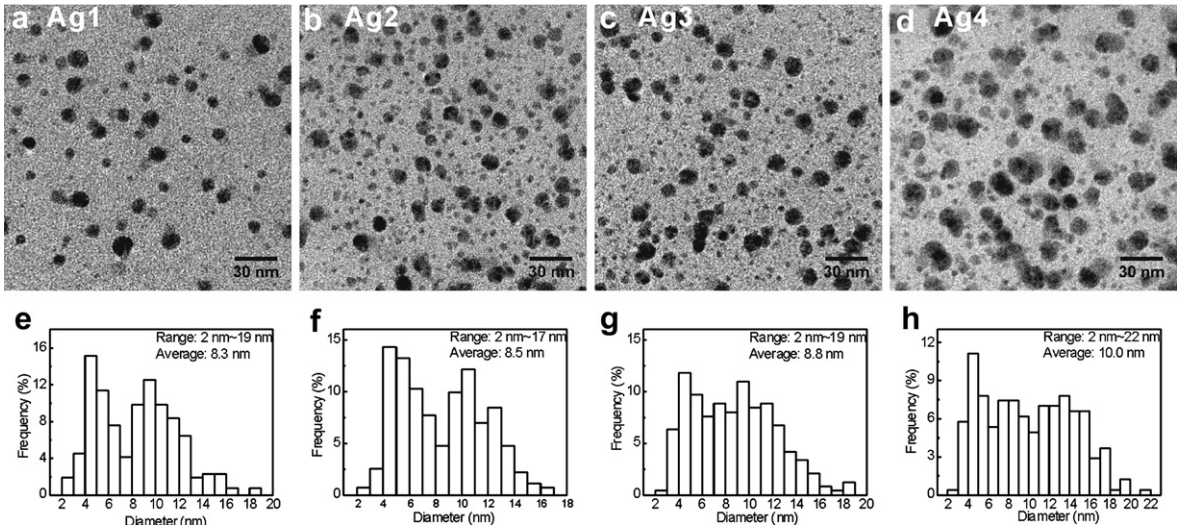

Fig. 1. TEM analysis of Ag/azopolymer composites. TEM images of (a) Ag1, (b) Ag2, (c) Ag3 and (d) Ag4. The scale bars are 30 nm. Particle size distribution histograms calculated from the TEM images (e) Ag1, (f) Ag2, (g) Ag3 and (h) Ag4.

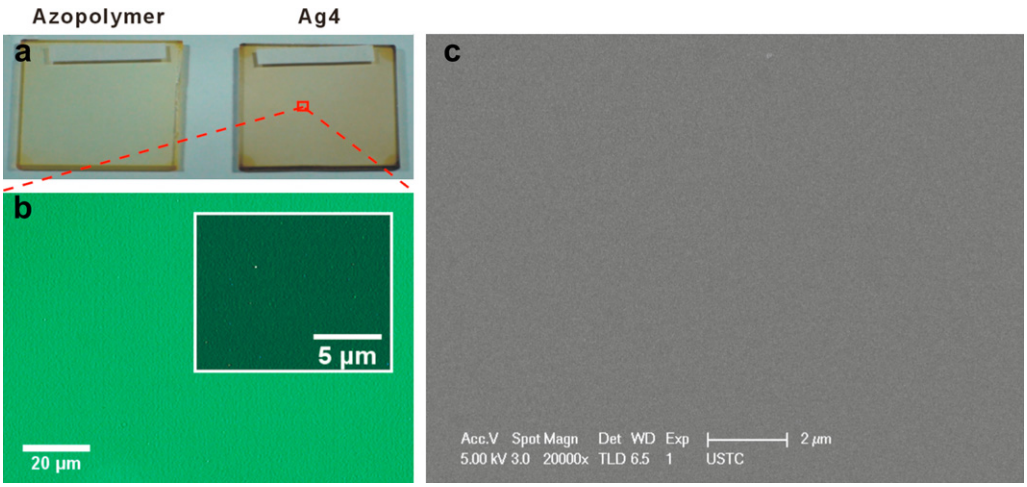

Fig. 2. (a) Photograph of the films of the nanocomposite Ag4; (b) Microscopic image of Ag4. Inset shows enlarged microscopic image of Ag4; (c) SEM image of Ag4.

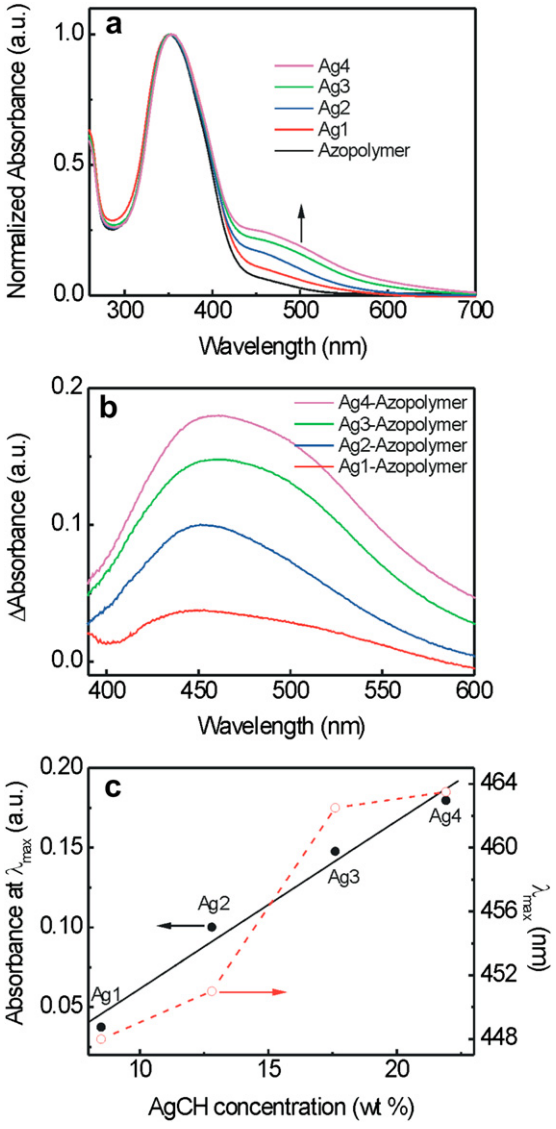

Fig. 3. (a) UV–vis absorption spectra of the azopolymer and the nanocomposite films; (b) UV–vis absorption spectra after subtraction of the absorbance of azopolymer from the measured absorption spectra; (c) λ_{max} and the absorbance at λ_{max} of the SPR bands as a function of the concentration of AgCH in the precursors.

which are shown in Fig. 3(b). The peaks of the SPR bands (λ_{max}) and the absorbance at λ_{max} are obtained from absorption spectra shown in Fig. 3(b) and the relationship between λ_{max}, the absorbance at λ_{max} and the concentration of AgCH in the precursors is shown in Fig. 3(c). For the absorbance at λ_{max}, results shown in Fig. 3(c) indicate that it increases linearly as the concentration of AgCH in the precursors increases. This result shows that the concentration of Ag nanoparticles in the nanocomposites can be well controlled by in situ synthesis. For λ_{max}, it also increases as the concentration of AgCH in the precursor increases. It is known that the SPR band of Ag nanoparticles red shifts as the size of Ag nanoparticles increases [34–36]. The result shown in Fig. 3(c) indicates that the size of Ag nanoparticles increases as the concentration of AgCH in the precursor increases. This result is in accordance with the TEM observations that the average diameter of Ag nanoparticles increases as the concentration of AgCH in the precursor increases.

λ_{max} of SPR bands of Ag1, Ag2, Ag3 and Ag4 are located at about 448 nm, 451 nm, 462.5 nm and 463.5 nm, respectively. In general, well-dispersed spherical Ag nanoparticles with 10 nm of diameter in aqueous solution show a sharp SPR band at around 400 nm [37]. Compared with Ag nanoparticles well-dispersed in aqueous solution, the SPR bands of Ag nanoparticles in the nanocomposite films are red-shifted and broadened. Many groups have reported that the SPR bands of Ag nanoparticles in thin films are red-shifted and broadened [38–46]. There are three reasons for the spectral changes:

1. Compared with Ag nanoparticles well-dispersed in solution, there are considerable interactions among Ag nanoparticles in thin films because they are close-packed [38–43]. Near-field coupling interactions of the more densely packed Ag nanoparticles cause red shift and broadening of the SPR band [38–43].
2. It is known that the SPR band of Ag nanoparticles is affected by the dielectric environment [35,36]. The refractive index of thin films is different from the aqueous solution. The refractive index of water is 1.33 and the refractive index of poly-(2-(4-cyanophenyl) diazenyl phenyloxy) ethoxyl methacrylate) (an azopolymer reported in the literature) is 1.682 [47]. So, different refractive indexes cause different SPR bands of Ag nanoparticles in the nanocomposite films and in aqueous solution [43–45].
3. According to the TEM analysis, the size distribution of the Ag nanoparticles is observed. Polydisperse samples show broad SPR bands.

Based on the results of TEM analysis and UV–vis spectroscopy, we conclude that Ag nanoparticles are formed in the azopolymer matrix.

In order to have a deeper understanding of the structure of the nanocomposites and the interactions between Ag and the azopolymer, the nanocomposites are investigated by XPS spectroscopy and FT-IR spectroscopy.

Since the Ag 3d regions of the XPS spectra are very sensitive to the environment of Ag [48–57], the reduction process was investigated by XPS. The Ag 3d XPS spectra and the binding energy of Ag $3d_{5/2}$ and $3d_{3/2}$ of Ag4 at different heating time at 95 °C are shown in Fig. 4. As the heating time increases, the Ag $3d_{5/2}$ and $3d_{3/2}$ peaks shift to lower binding energy. After 3 h heating, the Ag $3d_{5/2}$ and $3d_{3/2}$ peaks do not shift any more. This result indicates the reduction of Ag(I) is completed after heating for 3 h at 95 °C. The binding energy of Ag $3d_{5/2}$ and $3d_{3/2}$ after heating for 3 h are 367.7 eV and 373.75 eV, respectively, matching with the binding energy of Ag in zero oxidation state in polymer composites [48–50]. The binding energy of Ag $3d_{5/2}$ of Ag in zero oxidation state in polymer composites is usually lower than the pure Ag metal (368.3 eV) because interactions between Ag and polymer change the environment of Ag [48–50]. The most possible interactions between Ag and the azopolymer in the nanocomposites are Ag–N and Ag–O interactions.

It has been frequently pointed out that some substituent groups with N and O atoms have interactions with Ag nanoparticles [50–54]. We compare the N 1s and O 1s XPS spectra of the azopolymer without Ag and the nanocomposite Ag4. As shown in Fig. 5(a), the N 1s peak of poly(AzoCN-co-HEMA) is at 399.45 eV and the N 1s peak of Ag4 is at 400.00 eV. Chen et al. reported that the N 1s signal of coordinated N has larger binding energy than the signal of free N [52]. The result shown in Fig. 5(a) indicates that there is coordination interaction between N and Ag in the

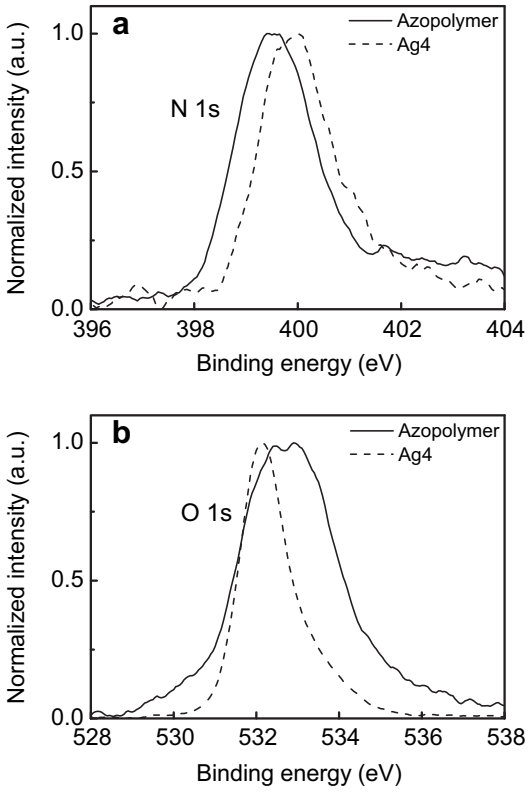

Fig. 5. (a) N 1s XPS spectra and (b) O 1s XPS spectra of the azopolymer poly(AzoCN-co-HEMA) and the nanocomposite Ag4.

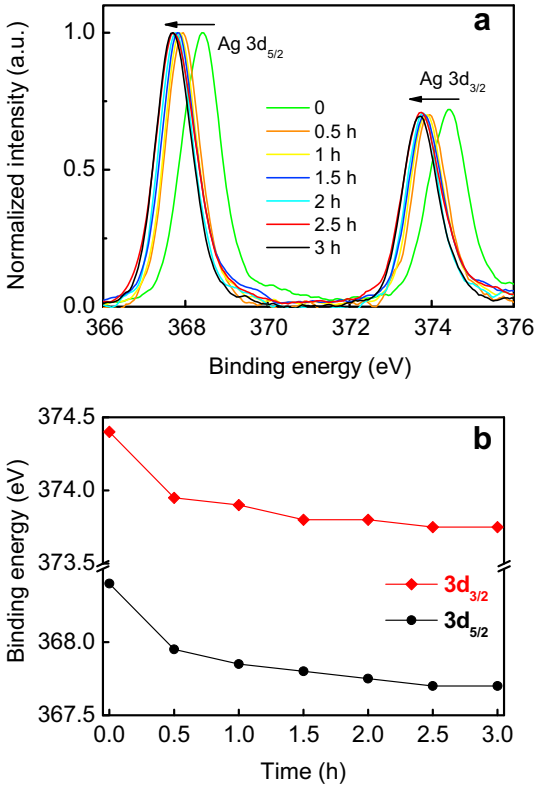

Fig. 4. (a) Ag 3d XPS spectra of Ag4 at different heating time; (b) Binding energy of Ag $3d_{3/2}$ and $3d_{5/2}$ as a function of the heating time.

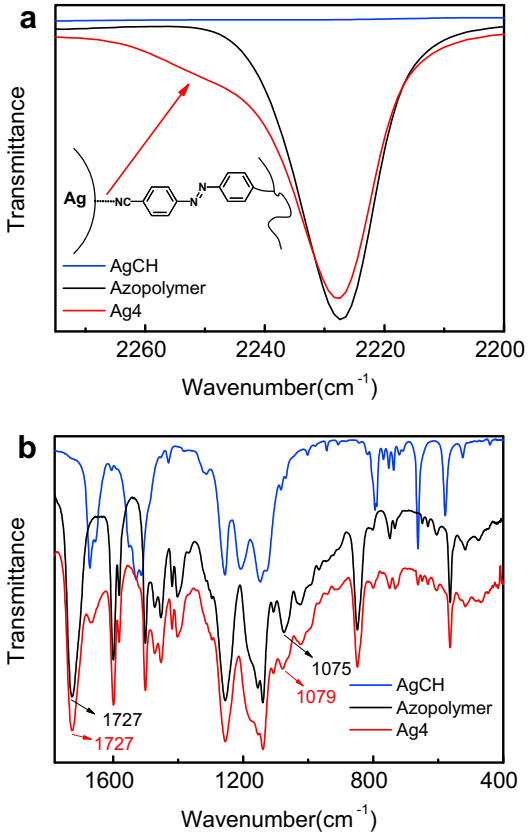

Fig. 6. FT-IR spectra of AgCH, poly(AzoCN-co-HEMA) and the nanocomposite Ag4.

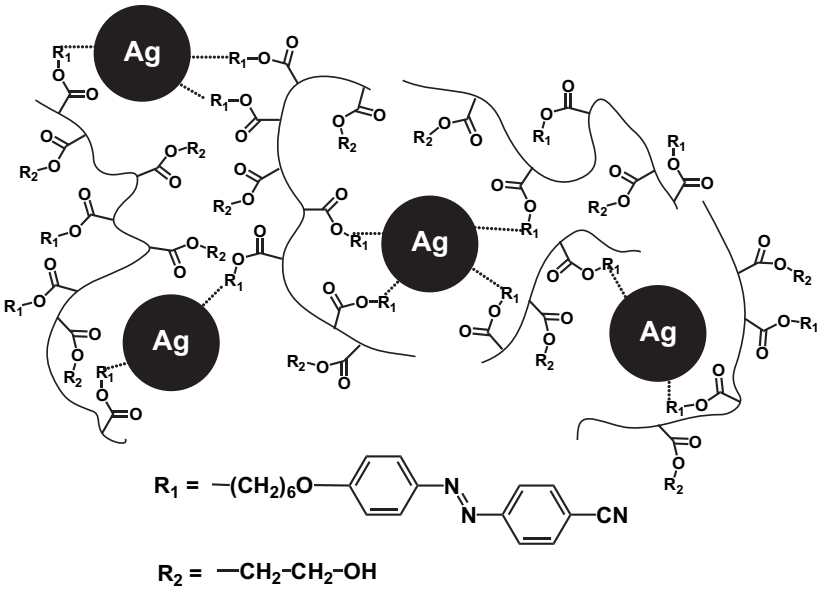

Scheme 2. Schematic model of the Ag/azopolymer nanocomposites.

nanocomposite [52]. There are two kinds of N atoms in the azopolymer. One is the N atom in the azo chromophore and the other is the N atom in the substituent nitrile group. Considering the possible coordination properties of the two kinds of N, the change of the N 1s peak is more possibly caused by the interaction between nitrile groups and Ag because nitrile groups have strong coordination interactions with Ag [32,58–60].

The coordination interaction between N and Ag is further studied by FT-IR spectroscopy. It is known that nitrile groups can in principle be bond to Ag via either its nitrogen lone pair electrons or its C≡N π system [32,58–60]. If nitrile coordinates with Ag via its nitrogen lone pair electrons, the nitrile triple bond vibrations will increase the stretching frequency; if nitrile coordinates with Ag via its π system, the nitrile triple bond vibrations will decrease the stretching frequency [58–60]. The FT-IR spectra of the poly(AzoCN-co-HEMA), AgCH and the nanocomposite Ag4 are shown in Fig. 6. As shown in Fig. 6(a), the band at around 2227 cm^{-1} is attributed to the C≡N triple bond vibrations. This band of poly(AzoCN-co-HEMA) is almost symmetric, but the C≡N band of Ag4 becomes asymmetric and a new shoulder at around 2250 cm^{-1} appears. Barmatov et al. reported that a new shoulder at 2246 cm^{-1} appears when nitrile groups coordinate with Ag nanoparticles [32]. Similar result reveals that there is coordination interaction between nitrile groups and Ag in the Ag/azopolymer nanocomposite. Compared with the peak at 2227 cm^{-1}, the shoulder at around 2250 cm^{-1} is shifted to higher stretching frequency, indicating the nitrile group coordinates with Ag via its nitrogen lone pair electrons. Since the signal at around 2250 cm^{-1} is weak, a control experiment was performed by using the homopolymer poly(6-(4-((4-cyanophenyl)diazenyl)phenoxy)hexyl methacrylate) (abbreviated as polyAzoCN) instead of the copolymer poly(AzoCN-co-HEMA) to form composites with Ag (More details in Supporting Information). The concentration of nitrile groups in the homopolymer is higher than those in the copolymer and we observe a more obvious shoulder at around 2250 cm^{-1} in the FT-IR spectrum of Ag/polyAzoCN.

Another possible type of interaction between Ag nanoparticles and the azopolymer is the Ag–O interaction, which is also studied by XPS. As shown in Fig. 5(b), compared with the O 1s signal of poly(AzoCN-co-HEMA), the O 1s signal of the nanocomposite Ag4 shifts to lower binding energy. Rubira et al. have reported similar changes of O 1s signal when they study Ag/polyimide composites [53]. It is known that both ester groups and hydroxyl groups may have interactions with Ag [50,51,61,62]. The change of O 1s signal could be due to the interactions between ester groups and Ag or hydroxyl groups and Ag. The Ag–O interactions are further studied by FT-IR spectra, which are shown in Fig. 6(b). The C=O bands in both the azopolymer and Ag4 are located at 1727 cm^{-1}. The C–O

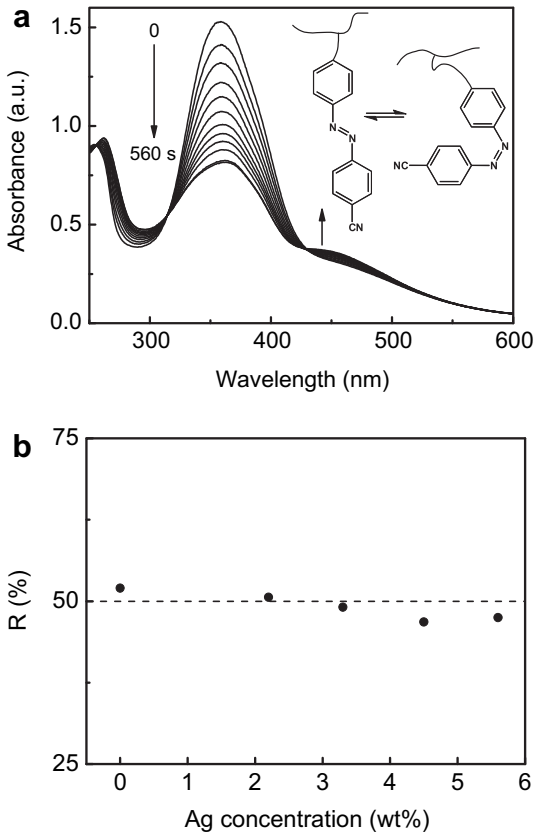

Fig. 7. (a) UV–vis absorption spectra of Ag3 under the irradiation of UV light at 365 nm. The spectra were recorded at different irradiation time. (b) The degree of photoisomerization *R* of the azopolymer and the nanocomposites.

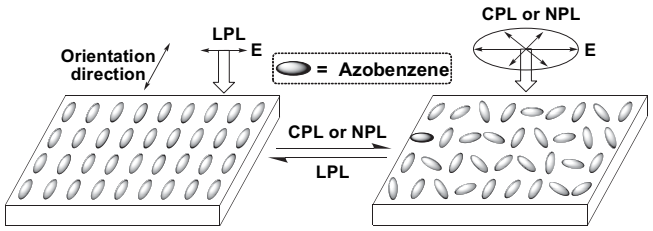

Scheme 3. Schematic model of reversible photo-induced orientation of azobenzene groups.

band in $-CH_2-OH$ group of the azopolymer and Ag4 are located at 1075 and 1079 cm^{-1}, respectively. There is not very obvious change of the signals of ester groups and hydroxyl groups in the FT-IR spectra. There are two possible reasons. One is that ester groups and hydroxyl groups are physically but not chemically adsorbed on the surface of Ag. The other is that only a small amount of ester groups and hydroxyl groups are chemically adsorbed on the surface of Ag and the signals are too weak to be detected by FT-IR.

Based on the results of XPS spectroscopy and FT-IR spectroscopy, we conclude that poly(AzoCN-co-HEMA) has interactions with Ag. Ag nanoparticles and poly(AzoCN-co-HEMA) form inorganic–organic nanocomposites. The schematic model of the nanocomposites is shown in Scheme 2.

3.2. Photoisomerization and optically induced and erased birefringence of Ag/azopolymer nanocomposites

It is reported that the photoisomerization of azobenzene groups are not prominent if azobenzene groups are covalently linked to the surfaces of noble metal because azobenzene groups form close-packed structures on the surfaces of noble metal so that there is not enough space for the movement of azobenzene groups [25,63]. In the Ag/azopolymer nanocomposites, Ag nanoparticles may affect photoisomerization of azobenzene groups. Fig. 7(a) shows the UV–vis absorption spectra of Ag3 at different time upon irradiation with UV light at 365 nm. The π–π^* transition band of trans isomers with λ_{max} at 358 nm decreases remarkably and, at the same time, the n–π^* transition band of cis isomers at around 455 nm increases slightly. The change of absorption bands in Fig. 7(a) and the presence of two isobestic points indicate that trans–cis isomerization happens in the nanocomposite without any other side reaction [9]. After irradiation for 560 s, the UV–vis spectra of Ag3 do not change any more, indicating azobenzene groups change to a cis saturated state. This photoisomerization is reversible and, after irradiation, the nanocomposite slowly recovers its initial absorption feature when it is kept in dark for a week.

The degree of photoisomerization R is estimated from the following equation [64]:

$$R = (A_0 - A_\infty)/A_0 \times 100\% \quad (1)$$

where A_0 and A_∞ are the initial absorbance and absorbance at the photostationary state of azobenzene groups at λ_{max}. The degree of photoisomerization of the nanocomposites with different concentration of Ag nanoparticles are measured and shown in Fig. 7(b). R changes from 52% to 47% as the content of Ag increases. R only slightly decreases as the concentration of Ag nanoparticles increases. This result indicates Ag nanoparticles do not strongly hinder the photoisomerization of azobenzene groups in the nanocomposites. According to the FT-IR spectrum shown in Fig. 6(a), both free azobenzene groups and azobenzene groups coordinated with Ag via nitrile–Ag interaction can be detected. So, not all the azobenzene groups are densely packed around Ag nanoparticles and the mobility of the azobenzene groups is not strongly hindered by Ag.

The optically rewritable property of Ag/azopolymer nanocomposites is studied by repeated optically induced and erased birefringence. It is known that azobenzene groups can be oriented using linearly polarized light (LPL), and circularly polarized light (CPL) or nonpolarized light (NPL) can randomize the chromophore orientations [7]. The schematic model of the reversible photo-induced orientation of azobenzene groups is shown in Scheme 3. In our experiment, the films are under the irradiation of LPL at 442 nm for 500 s and then the films are under the irradiation of CPL at 442 nm for 200 s. The irradiation lasts for 5 cycles for each sample.

Fig. 8(a) shows the transmittance (result from optical birefringence) changes of poly(AzoCN-co-HEMA) under light irradiation. During the first 500 s irradiation by LPL, the transmittance increases, indicating poly(AzoCN-co-HEMA) changes from an isotropic state to an orientated state. Then the transmittance decreases rapidly when poly(AzoCN-co-HEMA) is under the irradiation of CPL for 200 s. This result indicates that the oriented alignment of azobenzene groups is optically "erased" by overwriting the sample with CPL. As the cycles of repeated writing–erasing increases, the transmittance after LPL irradiation for 500 s gradually decreases. After 5 cycles of the repeated writing–erasing, there is 9.7% decrease of the transmittance, indicating the photo-induced alignment in the azopolymer film is not stable enough under the repeated writing–erasing processes. It is known the rewritable property of azopolymer is very important for the application as rewritable storage media [7–9]. The introduction of Ag into the azopolymer improves the rewritable property of the azopolymer and the results are discussed below.

Fig. 8(b) shows the transmittance change of Ag3 under light irradiation. Ag3 shows similar photo-induced orientation properties of poly(AzoCN-co-HEMA). However, after 5 cycles repeated writing–erasing process, there is only 2.9% decrease of the transmittance, indicating that the rewritable property of Ag3 is better than that of poly(AzoCN-co-HEMA). The transmittances of the

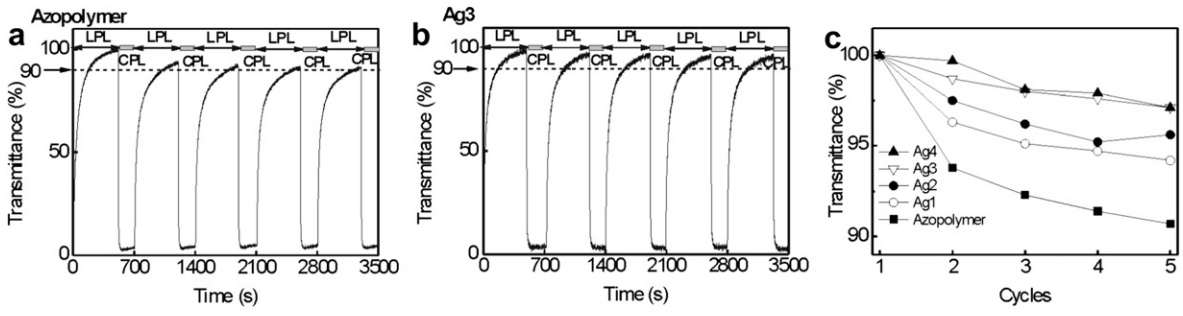

Fig. 8. Transmittance changes as a function of irradiation time of (a) Ag0 and (b) Ag3. The dashed lines in (a) and (b) are transmittance at 90%. (c) Transmittances of the samples after LPL irradiation for 500 s in every irradiation cycle.

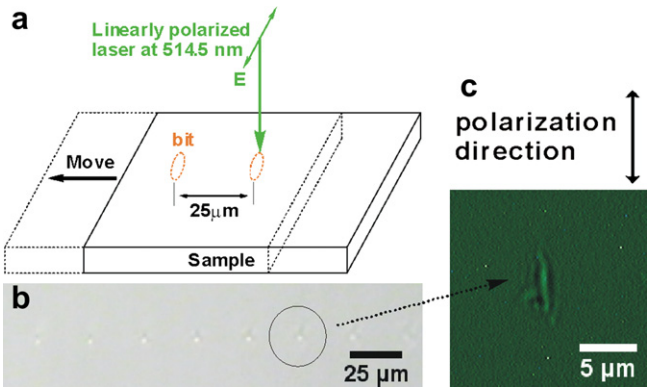

Fig. 9. (a) Schematic diagram for the one-photon optical recording experiment. (b) Microscopic image of the recorded data points on Ag4. (c) High resolution microscopic image of the recorded data point.

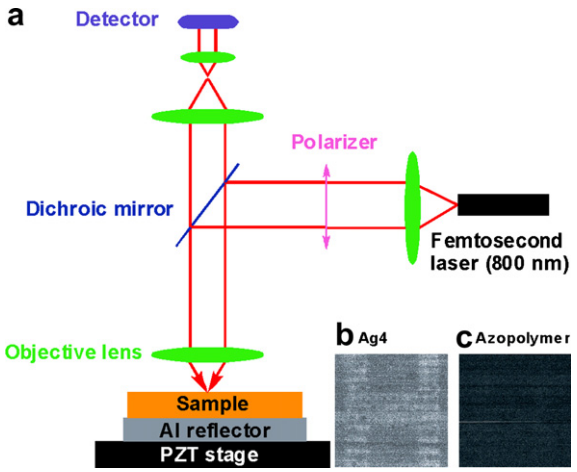

Fig. 10. (a) Schematic diagram of the two-photon recording experimental setup; (b) Microscopic image of a letter "H" recorded on Ag4; (c) Microscopic image of azopolymer. Image area of (b) and (c): 93 × 93 μm.

nanocomposites with different concentrations of Ag after LPL irradiation for 500 s in every irradiation cycle are shown in Fig. 8(c). An improvement of the rewritable property under repeated writing–erasing process is observed with an increase of Ag concentration.

There are two possible contributions for the improved optically rewritable property of the nanocomposites. Firstly, it is well known that crosslinking can enhance the stability of optically induced birefringence of azo chromophores [14,15,65,66]. As shown in Scheme 2, the chain-segments of poly(AzoCN-co-HEMA) are attached to Ag nanoparticles. Poly(AzoCN-co-HEMA) and Ag nanoparticles form a network-like structure which provides improved stability of the nanocomposites. Secondly, the filler reinforcement effect of Ag is commonly observed in nanocomposites [67]. Natural materials such as bone and shell and man-made composite materials that combine hard and soft materials can result in composite materials with improved mechanical properties and thermal stabilities [1–5]. In the Ag/azopolymer nanocomposites, Ag nanoparticle is a kind of "hard" inorganic material and azopolymer is a kind of "soft" polymeric material. The Ag/azopolymer system is just like combining hard and soft materials. This way, an improved stability can result.

3.3. *One-photon and two-photon optical recording of the Ag/azopolymer nanocomposites*

It is well known that image recording is one of the most promising applications of azopolymers [7–9]. Different from the normal azopolymer systems, the nanocomposites are with a high concentration of Ag nanoparticles. Are there any effects of Ag nanoparticles on the image recording of azopolymer? To answer this question, both one-photon and two-photon technologies are used to record data points on the nanocomposites.

In one-photon recording experiment, we use a linearly polarized laser at 514.5 nm and a mobile sample stage to record data points on Ag4. The schematic diagram of the one-photon optical recording experiment is shown in Fig. 9(a). As shown in Fig. 9(b), some data points appear after the recording process. We obtain a high resolution microscopic image of a recording data point by using an Olympus U-TP530 tint plate and WT-MV3100G software. As shown in Fig. 9(c), the data point is not round but an elliptical point which is prolonged along the polarization direction. It is known that mass transfer along the polarization direction will happen if an azopolymer is under irradiation of linearly polarized light [7,68,69]. From the observation on Fig. 9(c), it can be deduced that photo-induced mass transfer happens in Ag4. This result is in accordance with the result of photoisomerization and shows again that the mobility of azobenzene groups is not strongly hindered by Ag nanoparticles. So, the nanocomposites are suitable for the fabrication of microstructures such as surface-relief-gratings which need photo-induced mass transfer.

Optical recording of Ag/azopolymer nanocomposites was also performed by two-photon technology. The schematic diagram of the two-photon recording experiment is shown in Fig. 10(a). As shown in Fig. 10(b), a letter "H" is recorded on Ag4 by two-photon technology with the recording power of 6 mW. Under the same recording condition, we have tried to record a letter on the azopolymer film without Ag nanoparticles. However, no two-photon image can be observed on the azopolymer without Ag nanoparticles. In our previous work, using the same two-photon recording setup, the recording threshold value for bisazobenzene polymer is about 12 mW [31]. Obviously, the Ag/azopolymer nanocomposite has a lower two-photon recording threshold value than the bisazobenzene polymer. It is well known that Ag nanoparticles may largely enhance the two-photon absorption and emission of dyes near Ag nanoparticles [70]. Very recently, Tusboi et al. demonstrated that photochromism is promoted by two-photon absorption due to an enhanced electronic field (localized surface plasmon) of noble metal nanoparticles [71]. It was argued that there is energy transfer between Ag nanoparticles and azobenzene groups [19]. The possible reason for the low two-photon recording power of Ag4 is that Ag nanoparticles have an enhancement effect on the two-photon absorption of azobenzene groups. The details of the effect of Ag nanoparticles on the two-photon absorption of azobenzene needs further study.

4. Conclusions

In summary, in situ synthesized Ag/azopolymer nanocomposites with controlled and high concentration of Ag nanoparticles have been prepared. Homogeneous and highly transparent nanocomposites with 2.2–5.6 wt% Ag are obtained. Ag nanoparticles and azopolymers form a network-like structure via the Ag–polymer interactions and the optically rewritable property of the nanocomposites is enhanced. Photoisomerization and one-photon recording experiment show that the movement of azobenzene groups in the nanocomposites is not strongly hindered by Ag nanoparticles. The newly synthesized polymer nanocomposites also show two-photon recording property with a recording power

as low as 6 mW. The nonlinear optical properties of the nanocomposites are expected to be very interesting because both Ag nanoparticles and azobenzene groups show nonlinear optical properties. The effect of SPR of Ag nanoparticles on the nonlinear optical properties of azopolymer is the focus of our current effort.

Acknowledgement

This work is supported by National Natural Science Foundation of China (No. 50703075, 50773075, 50533040 and 50875251), the Chinese Academy of Sciences (kjcx3.sywH02 and kjcx2-yw-m11), and National Basic Research Program of China (No. 2006cb302900). The authors thank J. Zuo (USTC) for the one-photon recording experiment.

Appendix. Supplementary material

Supplementary material associated with this article can be found in the on-line version, at doi:10.1016/j.polymer.2010.01.062.

References

[1] Balazs AC, Emrick T, Russell TP. Science 2006;314:1107–10.
[2] Nguyen TQ, Wu J, Doan V, Schwartz BJ, Tolbert SH. Science 2000;288:652–6.
[3] Lu Y, Yang Y, Sellinger A, Lu M, Huang J, Fan H, et al. Nature (London) 2001;410:913–7.
[4] Podsiadlo P, Kaushik AK, Arruda EM, Waas AM, Shim BS, Xu J, et al. Science 2007;318:80–3.
[5] Capadona JR, Shanmuganathan K, Tyler DJ, Rowan SJ, Weder C. –. Science 2008;319:1370–4;
Diaconu G, Paulis M, Leiza JR. Polymer 2008;49:2444–54.
[6] Delaire JA, Nakatani K. Chem Rev 2000;100:1817–45.
[7] Natansohn A, Rochon P. Chem Rev 2002;102:4139–75.
[8] Yu Y, Ikeda T. J Photochem Photobiol C 2004;5:247–65;
Wang D, Liu J, Ye G, Wang X. Polymer 2009;50:418–27.
[9] Shibaev V, Bobrovsky A, Boiko N. Prog Polym Sci 2003;28:729–836.
[10] Mikami R, Taguchi M, Yamada K, Suzuki K, Sato O, Einaga Y. Angew Chem Int Ed 2004;43:6135–9.
[11] Suda M, Nakagawa M, Iyoda T, Einaga Y. J Am Chem Soc 2007;129:5538–43;
Suda M, Kameyama N, Suzuki M, Kawamura N, Einaga Y. Angew Chem Int Ed 2008;47:160–3.
[12] Bo Q, Yavrian A, Galstian T, Zhao Y. Macromolecules 2005;38:3079–86;
Dahmane S, Zhao Y. J Appl Polym Sci 2006;102:744–50;
Dahmane S, Lasia A, Zhao Y. Macromol Chem Phys 2006;207:1485–91;
Cui L, Dahmane S, Tong X, Zhu L, Zhao Y. Macromolecules 2005;38:2076–84.
[13] Li X, Chon JWM, Evans RA, Gu M. Appl Phys Lett 2008;92:063309.
[14] Kulikovska O, Goldenberg LM, Kulikovsky L, Stumpe J. Chem Mater 2008;20:3528–34.
[15] Kulikovska O, Goldenberg LM, Stumpe J. Chem Mater 2007;19:3343–8.
[16] Nishizawa K, Nagano S, Seki T. Chem Mater 2009;21:2624–31.
[17] Hubert C, Rumyantseva A, Lerondel G, Grand J, Kostcheev S, Billot L, et al. Nano Lett 2005;5:615–9.
[18] Zhou J, Yang J, Sun Y, Zhang D, Shen J, Zhang Q, et al. Thin Solid Films 2007;515:7242–6.
[19] Ahonen P, Schiffrin DJ, Paprotny J, Kontturi K. Phys Chem Chem Phys 2007;9:651–8.
[20] Zhang A, Fang Y. Chem Phys 2006;331:55–60.
[21] Vlčková B, Moskovits M, Pavel I, Šišková K, Sládková M, Šlouf M. Chem Phys Lett 2008;455:131–4.
[22] Gao J, Sun Y, Zhou J, Zheng Z, Chen H, Su W, et al. J Polym Sci Part A Polym Chem 2007;45:5380–6.
[23] Klajn R, Wesson PJ, Bishop LJM, Grzybowski BA. Angew Chem Int Ed 2009;48:7035–9.
[24] Sidhaye DS, Kashyap S, Sastry M, Hotha S, Prasad BLV. Langmuir 2005;21:7979–84.
[25] Evans SD, Johnson SR, Ringsdorf H, Williams LM, Wolf H. Langmuir 1998;14:6436–40.
[26] Callari F, Petralia S, Sortino S. Chem Commun; 2006:1009–11.
[27] Manna A, Chen P-L, Akiyama H, Wei T-X, Tamada K, Knoll W. Chem Mater 2003;15:20–8.
[28] Ishitobi H, Tanabe M, Sekkat Z, Kawata S. Appl Phys Lett 2007;91:091911.
[29] Liu J, Sun K, Li Z, Gao J, Su W, Yang J, et al. Polymer 2004;45:4331–6.
[30] Wu S, Yu X, Huang J, Shen J, Yan Q, Wang X, et al. J Mater Chem 2008;18:3223–9.
[31] Zhang Z, Hu Y, Luo Y, Zhang Q, Huang W, Zou G. Opt Commun 2009;282:3282–5;
Hu Y, Zhang Z, Lei S, Ding J, Xu M, Huang W, et al. Proc SPIE 2008;7125:71250Y.
[32] Barmatov EB, Pebalk DA, Barmatova MV. Langmuir 2004;20:10868–71.
[33] Giuffrida S, Ventimiglia G, Sortino S. Chem Commun; 2009:4055–7.
[34] Link S, El-Sayed MA. J Phys Chem B 1999;103:8410–26.
[35] Kelly KL, Coronado E, Zhao LL, Schatz GC. J Phys Chem B 2003;107:668–77.
[36] Noguez C. J Phys Chem C 2007;111:3806–19.
[37] Cañamares MV, Garcia-Ramos JV, Gómez-Varga JD, Domingo C, Sanchez-Cortes S. Langmuir 2005;21:8546–53;
Henglein A, Giersig M. J Phys Chem B 1999;103:9533–9.
[38] Atay T, Song J-H, Nurmikko AV. Nano Lett 2004;4:1627–31.
[39] Kim WS, Jia L, Thomas EL. Adv Mater 2009;21:1921–6.
[40] Bockstaller MR, Mickiewicz RA, Thomas EL. Adv Mater 2005;17:1331–49;
Bockstaller MR, Thomas EL. J Phys Chem B 2003;107:10017–24.
[41] Wang W, Chen X, Efrima S. J Phys Chem B 1999;103:7238–46.
[42] Selvakannan PR, Swami A, Srisathiyanarayanan D, Shirude PS, Pasricha R, Mandale AB, et al. Langmuir 2004;20:7825–36.
[43] Zhang L, Shen Y, Xie S, Li S, Jin B, Zhang Q. J Phys Chem B 2006;110:6615–20.
[44] Malynych S, Chumanov G. J Opt A Pure Appl Opt 2006;8:S144–7.
[45] Swami A, Selvakannan PR, Pasricha R, Sastry M. J Phys Chem B 2004;108:19269–75.
[46] Khanna PK, Singh N, Charan S, Subbarao VVVS, Gokhale R, Mulik UP. Mater Chem Phys 2005;93:117–21.
[47] Wang D, Zhang J, Ming H, Yan Q, Zhang Q, Wang P, et al. Chin Phys Lett 2004;21:2445–7.
[48] Shah MdS AS, Nag M, Kalagara T, Singh S, Manorama SV. Chem Mater 2008;20:2455–60.
[49] Thiel J, Pakstis L, Buzby S, Raffi M, Ni C, Pochan DJ, et al. Small 2007;3:799–803.
[50] Gao Y, Jiang P, Liu DF, Yuan HJ, Yan XQ, Zhou ZP, et al. J Phys Chem B 2004;108:12877–81.
[51] Huang HH, Ni XP, Loy GL, Chew CH, Tan KL, Loh FC, et al. Langmuir 1996;12:909–12.
[52] Chen C-W, Serizawa T, Akashi M. Langmuir 1999;15:7998–8006.
[53] Rubira AF, Rancourt JD, Caplan ML, St Clair AK, Taylor LT. Chem Mater 1994;6:2351–8.
[54] Wang Y, Li Y, Yang S, Zhang G, An D, Wang C, et al. Nanotechnology 2006;17:3304–7.
[55] Rybak BM, Ornatska M, Bergman KN, Genson KL, Tsukruk VV. Langmuir 2006;22:1027–37.
[56] He S, Yao J, Xie S, Pang S, Gao H. Chem Phys Lett 2001;343:28–32.
[57] Chastain J. Handbook of X-ray photoelectron spectroscopy. 2nd ed. Eden Prairie: Perkin–Elmer Corporation (Physical Electronics Division); 1992.
[58] Park SH, Kim K, Kim MS. J Mol Struct 1993;301:57–64;
Storhoff BN, Lewis HC. Coord Chem Rev 1977;23:1–29.
[59] Joo S-W, Chung TD, Jang WC, Gong M-s, Geum N, Kim K. Langmuir 2002;18:8813–6;
Bae SJ, Lee C-r, Choi IS, Hwang C-S, Gong M-s, Kim K, et al. J Phys Chem B 2002;106:7076–80;
Lee C-r, Bae SJ, Gong M-s, Kim K, Joo S-W. J Raman Spectrosc 2002;33:429–33.
[60] Son DH, Ahn SJ, Lee YJ, Kim K. J Phys Chem 1994;98:8488–93;
Muniz-Miranda M, Pergolese B, Bigotto A. J Phys Chem C 2008;112:6988–92.
[61] Mbhele ZH, Salemane MG, van Sittert CGCE, Nedeljković JM, Djoković V, Luyt AS. Chem Mater 2003;15:5019–24.
[62] Porel S, Singh S, Harsha SS, Rao DN, Radhakrishnan TP. Chem Mater 2005;17:9–12.
[63] Akiyama H, Tamada K, Nagasawa J, Abe K, Tamaki T. J Phys Chem B 2003;107:130–5.
[64] Deng Y, Li Y, Wang X. Macromolecules 2006;39:6590–8;
Li Y, Deng Y, Tong X, Wang X. Macromolecules 2006;39:1108–15.
[65] Takase H, Natansohn A, Rochon P. J Polym Sci Part B Polym Phys 2001;39:1686–96.
[66] Zhou J, Shen J, Yang J, Ke Y, Wang K, Zhang Q. Opt Lett 2006;31:1370–2;
Zhou J, Yang J, Ke Y, Shen J, Zhang Q, Wang K. Opt Mater 2008;30:1787–95.
[67] Gunawidjaja R, Jiang C, Peleshanko S, Ornatska M, Singamaneni S, Tsukruk VV. Adv Funct Mater 2006;16:2024–34.
[68] Bian S, Li L, Kumar J, Kim DY, Williams J, Tripathy SK. Appl Phys Lett 1998;73:1817–9.
[69] Li Y, He Y, Tong X, Wang X. J Am Chem Soc 2005;127:2402–3;
Deng Y, Li N, He Y, Wang X. Macromolecules 2007;40:6669–78.
[70] Wenseleers W, Stellacci F, Meyer-Friedrichsen T, Mangel T, Bauer CA, Pond SJK, et al. J Phys Chem B 2002;106:6853–63;
Gryczynski I, Malicka J, Shen Y, Gryczynski Z, Lakowicz JR. J Phys Chem B 2002;106:2191–5.
[71] Tsuboi Y, Shimizu R, Shoji T, Kitamura N. J Am Chem Soc 2009;131:12623–7.